

Enhanced cation-substituted p-type doping in GaP from dual surfactant effects

Junyi Zhu*, Feng Liu, G.B. Stringfellow

University of Utah, USA

ARTICLE INFO

Article history:

Received 1 June 2009

Received in revised form

28 August 2009

Accepted 14 October 2009

Communicated by R.M. Biefeld

Available online 1 November 2009

PACS:

68.35.-p

68.43.Bc

81.05.Ea

68.55.Ln

Keywords:

A1. Doping

A1. Surface

A3. Organometallic vapor phase epitaxy

B2. Semiconducting III–V materials

ABSTRACT

We report first principles calculations demonstrating a dual-surfactant effect of Sb and H on enhanced Zn, Mg, Be and Cd incorporation in organometallic vapor phase epitaxially grown GaP films. The combined effects of Sb and H lower significantly the film doping energy during the epitaxial growth of all the p-type dopants studied, while neither Sb nor H can work alone as effectively. The role of H is to satisfy the electron counting rule. The role of Sb is to serve as an electron reservoir to help electron redistribution. We also predict that due to the low electronegativity of Mg, Sb and H will enhance Mg doping the least among these dopants because Mg as an electron reservoir itself may negate the electron reservoir effect of Sb. Our findings provide an important general physical understanding for p-type doping in III–V thin films.

Published by Elsevier B.V.

In epitaxial growth, surfactants have been proved to be effective to control the thin film microstructure, composition and morphology and hence to improve the thin film properties and device performance. Copel et al. in 1989 first used As as a surfactant in the growth of Si/Ge/Si(001) to suppress island formation [1]. Surfactant effects may affect crystal growth in various ways: (1) they can change the growth mode. In addition to Copel's work [1], the growth mode of Ag on Ag(111) is also changed when Sb is used as a surfactant [2,3]. (2) Surfactants can reduce interface roughness. For example, Bi as a surfactant reduces the surface roughness of InGaAs grown on GaAs substrates [4]. (3) Interface alloy intermixing can be suppressed by surfactants. For example, H can suppress the interface intermixing of Ge(001) covered Si [5]. (4) They can be used to change the surface reconstruction and, hence, induce the formation of various new ordered phases. For example, Sb is known to suppress Cu–Pt ordering in GaInP [6]. At higher concentrations, it can change the surface reconstruction from (2×4) to (2×3) -like inducing a new ordered phase in InGaP [6]. (5) Surfactants can also strongly affect the incorporation of dopants in semiconductors [7,8]. This last effect will be the focus of this paper.

* Corresponding author.

E-mail address: zhu@eng.utah.edu (J. Zhu).

The surfactant effects listed above may be attributed to several physical mechanisms. Surfactants can change the growth thermodynamics, by altering the surface energy. For example, surface As is known to lower the surface energy of the Si/Ge/Si system to suppress island formation [1]. In addition to changing the thermodynamics, surfactants can also change the growth kinetics, such as surface diffusion [2] and the size of step-edge barriers [3]. For example, Sb as a surfactant has been shown to reduce the mobility of Ag adatoms. This results in a higher island density leading to a change of growth mode. Sb as a surfactant on Ag(111) or GaAs can also reduce the step edge barrier and promote smoother growth morphologies [3,9].

Obtaining high doping levels in high bandgap materials has been a difficult problem for decades. This hinders high-level p-type doping in III–V materials such as phosphide and nitride semiconductors. This may be caused by several factors, including the limited solubility of acceptors, H passivation of acceptors, and high acceptor-hole binding energies [10,11]. An effective approach to achieving high p-type doping levels in GaInP, GaP, and GaAs employs the use of surfactants during organometallic vapor-phase epitaxy (OMVPE) growth [6–8]. For example, a recent study showed that Sb can be used to enhance the incorporation of dopants, such as Zn [7,8], and reduce unintentional impurities, such as C, S, and Si [8]. In addition to Sb, surface H was postulated to also play a role in the doping process [7,8]. The enhanced Zn

doping was speculated to be caused by kinetic and/or thermodynamic factors. The presence of Sb may increase the surface diffusion of Zn and allow more Zn to reach step edges and incorporate into the film [12]. Also, the neutral Zn–H complexes have a lower film doping energy than the isolated Zn [7]. However, there remains insufficient understanding of the underlying doping mechanisms associated with surfactants because it is impossible to directly observe the microscopic doping process.

A surfactant in epitaxial growth is defined as an active element that floats on top of the growing film surface. It is usually a single foreign element. Recently, we introduced a “dual-surfactant” effect, for which the surfactants can assist p-type doping of the epitaxial film only when two foreign surface elements are present while neither of the two can act alone to assist doping [13]. Specifically, we studied theoretically the doping process of Zn in GaP and found that the combined effects of Sb and H lower significantly the Zn film doping energy, while neither Sb nor H can work alone as effectively. Here, we use the term “film” doping energy as the energy change for a dopant atom (such as Zn) replacing a cation atom (such as Ga) in the subsurface position during epitaxial growth process to differentiate from the “bulk” doping energy for a dopant atom replacing a cation atom in the bulk. In this paper, we report the results of an investigation of the possible dual surfactant effects of Sb and H on the incorporation of other p-type dopants sitting on the Ga sublattice in GaP.

We have carried out extensive first-principles calculations of Zn, Mg, Be and Cd incorporation in (001) GaP films under the influence of surface Sb and H. We found that Sb alone has little effect on the film doping energy of all the dopants in GaP film, and it is only when H is also present that the film doping energy is substantially lowered by Sb. Also, surface H does not function as effectively alone without Sb. It is, thus, the combined effect of Sb and H that makes the p-type doping processes thermodynamically favorable. The role of Sb is to serve as an electron reservoir to accommodate the redistribution of electrons, in a similar spirit to the generalized electron counting rule (ECR) in the semiconductor surface with metal elements [14]. The role of H is to supply the one electron missing from the p-type dopant, so that the system can satisfy the ECR [15]. Experimentally, it is difficult to achieve high doping levels of Mg and Zn in III–V systems [8,16]. Our findings may illustrate an important theoretical insight and suggest a common strategy for improved p-type doping during epitaxial growth in all III–V compounds.

Our calculations were performed using the Vienna *ab initio* simulation package [17] within the local density approximation. We model the GaP (001) films by the same technique as we applied in our previous calculation on the dual surfactant effect of Sb and H on Zn in GaP [13].

In our calculation, we chose the (2 × 2) reconstructed surface as shown in Fig. 1, as explained in reference [13]. To obtain the film doping energy during epitaxial growth, we replace one Ga atom in the first (Fig. 2) or second (Fig. 3) cation layer with a p-type dopant atom and calculate the energy difference between the doped system and the undoped system. The effect of surfactant Sb on the film doping energy was calculated by

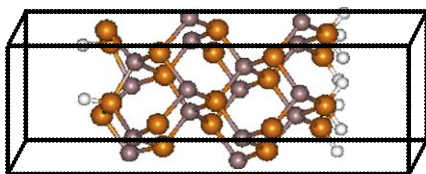


Fig. 1. Schematics of GaP supercell slab. Large orange sphere: P; small wine sphere: Ga; smallest white sphere: H. (For interpretation of the references to color in this figure legend, the reader is referred to the web version of this article.)

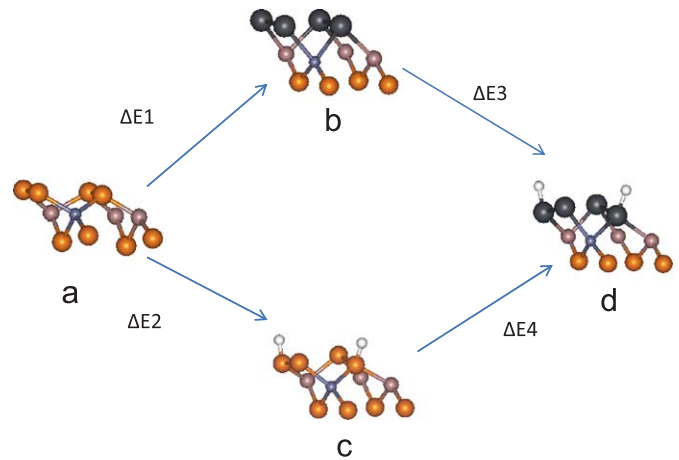


Fig. 2. Schematic illustration of various doping configurations, with one p-type dopant atom replacing a Ga atom in the first cation layer. ΔE indicates the change of film doping energy from one configuration to another indicated by the arrows. Largest (black) sphere: Sb; large (orange) sphere: P; medium (wine) sphere: Ga; small (blue): p-type dopant; smallest (white) sphere: H. (For interpretation of the references to color in this figure legend, the reader is referred to the web version of this article.)

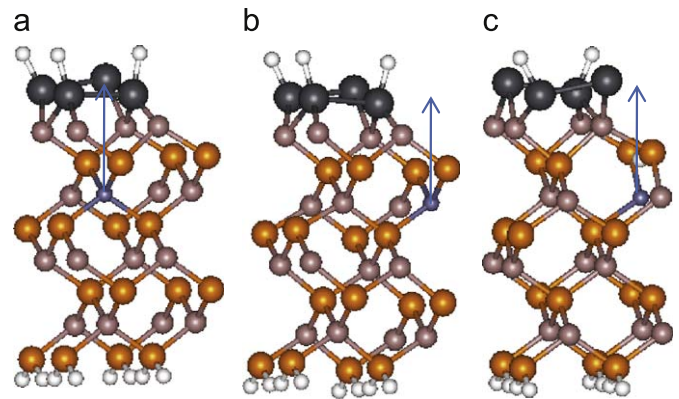


Fig. 3. (Color online) Ball-stick schematic illustration of one p-type dopant atom doped in the second cation layer. Atom labels are the same as in Fig. 2. (a) Dopant atom doped at the site between two surface dimers with three surface H. (b) Dopant atom doped at the site below a surface dimer with three surface H. (c) Dopant atom doped at the site between two surface dimers with two surface H and one bulk H next to dopant. (The arrows indicate the position of the dopant atom relative to the surface dimer.)

replacing surface P dimers with Sb dimers, assuming the surface reconstruction remains the same [20]. The effect of H as the second surfactant was studied by introducing different concentrations and configurations of H on the surface. The film doping energy is defined as

$$\Delta E_{\text{doping}} = E_{\text{doped}} - E_{\text{undoped}} + \mu_{\text{Ga}} - \mu_{\text{Dopant}}, \quad (1)$$

where E_{doped} (E_{undoped}) is the total energy of the doped (undoped) system, i.e. supercell; μ_{Ga} (μ_{Dopant}) is the chemical potentials of Ga (dopant). In general, μ_{Ga} may vary from $\mu_{\text{Ga}}[\text{bulk}] + \Delta H_f[\text{GaP}]$ (the P-rich condition) to $\mu_{\text{Ga}}[\text{bulk}]$ (the Ga-rich condition) [21], where $\Delta H_f[\text{GaP}]$ is the GaP enthalpy of formation; μ_{Dopant} equals $\mu_{\text{Dopant}}[\text{bulk}]$. In calculating the change of film doping energy due to surfactant Sb, μ_{Ga} and μ_{Zn} do not appear. In the case of H, the film doping energy depends on the chemical potential of H (μ_{H}) if one additional H is added to the system upon doping. The chemical potential of H is a variable strongly depending upon the growth condition. Here, we choose the typical value of $\mu_{\text{H}} = -0.67$ eV, one-half of the energy of an H_2 molecule at

$T = 900\text{ K}$, $p = 1\text{ atm}$ [22]. We stress that this is different from the value we used in the original analysis [13], which would correspond to a H partial pressure of 10^{-10} atm , unrealistically low for the OMVPE growth. We further note that in the OMVPE growth, there is a large catalytic effect of the phosphide surface on the decomposition of precursors [23]. So the actual chemical potential of the atomic H may be difficult to estimate due to non-equilibrium conditions at the surface. The chemical potential given here in the gas phase may be considered as the lower limit, because the actual H chemical potential could be higher due to the surface adsorption and decomposition of the precursor [23]. This would lead to a larger doping energy drop due to the extra H than our estimation.

First, we studied the doping energy differences of bulk vs. film without surfactant. We calculated the p-type doping energy in bulk GaP as a reference. Then, we calculated the p-type film doping energy in the surface positions of a GaP (001) film, by replacing the Ga in the first cation layer (Fig. 2a). Also, to exclude the possible surfactant enhancement effect of H, we do not include H on the top of the (2×2) surface in this calculation. We obtained the bulk and film doping energies for Zn, Be, Mg, Cd shown in Table 1. The fourth column of Table 1 shows the doping energy difference for all the dopants between the film and bulk. We found the presence of the surface lowers the doping energy from 0.2 eV to about 1 eV in reference to bulk for different dopants. This difference is possibly due to the covalent radius difference. The covalent radius of Zn is very close to that of Ga and the covalent radius of Be is slightly smaller than that of Ga. Thus when Zn or Be is incorporated, the difference of doping energy in the bulk vs. in the film is small because of the small strain effect. In contrast, the covalent radii of Cd and Mg are larger than that of Ga, so the presence of surface in the film allows more strain relaxation to accommodate the large size of Cd and Mg, and hence to reduce noticeably the film doping energy relative to that in the bulk.

Next, we investigated the surfactant effect of Sb. When Sb is introduced during OMVPE growth, it stays on top of the surface replacing the P surface dimers, due to its large atomic size and lower dangling bond energy (see Fig. 2b). This has been demonstrated experimentally by surface photo reflection spectra [24] and is supported by first-principles calculations [20]. To exclude the possible surfactant enhancement effect of H, we at first did not include H on the surface. In our previous study of Zn doping, we replaced surface P dimers with Sb dimers without H (Fig. 2b) and obtained $\Delta E_{1st}^{Sb,Zn} = 2.53\text{ eV} + \mu_{Ga} - \mu_{Zn}$, which is 0.07 eV higher than the P dimer case [13]. This film doping energy difference is defined as ΔE_1 in Table 2. Here, we performed

Table 1
Doping energies of bulk and film without surfactant for different dopants.

	Bulk	Film	$E_{\text{Film}} - E_{\text{Bulk}}$ (eV)
Be	$0.23\text{ eV} + \mu_{Ga} - \mu_{Be}$	$0.02\text{ eV} + \mu_{Ga} - \mu_{Be}$	-0.21
Zn	$2.69\text{ eV} + \mu_{Ga} - \mu_{Zn}$	$2.46\text{ eV} + \mu_{Ga} - \mu_{Zn}$	-0.23
Mg	$2.61\text{ eV} + \mu_{Ga} - \mu_{Mg}$	$2.14\text{ eV} + \mu_{Ga} - \mu_{Mg}$	-0.47
Cd	$3.69\text{ eV} + \mu_{Ga} - \mu_{Cd}$	$2.74\text{ eV} + \mu_{Ga} - \mu_{Cd}$	-0.95

Table 2
Film doping energy difference for p-type dopants with different surface configurations in GaP as shown in Fig. 2.

	Zn	Mg	Cd	Be
ΔE_1 (eV)	0.07	-0.15	0.19	0.36
ΔE_2 (eV)	0.22	0.07	0.55	0.41
ΔE_3 (eV)	-0.78	-0.47	-0.49	-0.92
ΔE_4 (eV)	-0.93	-0.69	-0.85	-0.97

the same calculation for dopants Be, Mg and Cd, and obtained $\Delta E_{1st}^{Sb,Be} = 0.38\text{ eV} + \mu_{Ga} - \mu_{Be}$, $\Delta E_{1st}^{Sb,Mg} = 1.99\text{ eV} + \mu_{Ga} - \mu_{Mg}$ and $\Delta E_{1st}^{Sb,Cd} = 2.93\text{ eV} + \mu_{Ga} - \mu_{Cd}$, respectively. In comparison to the case of P surface dimers, the corresponding film doping energy changes are $\Delta E_1(\text{Be}) = 0.36\text{ eV}$, $\Delta E_1(\text{Mg}) = -0.15\text{ eV}$ and $\Delta E_1(\text{Cd}) = 0.19\text{ eV}$, as listed in Table 2. Importantly, we found that for all p-type dopants studied, the film doping energy difference, ΔE_1 (Fig. 2a vs. b), between the Sb dimer case and the P dimer case is nearly zero (Zn, Mg) or positive (Cd, Mg). This indicates that Sb alone does not significantly enhance the p-type doping of GaP without H.

Next, we studied the role of H in the doping process. OMVPE growth produces a large concentration of atomic H on the surface [23]. A significant concentration of H (presumably in the form of Zn-H and C-H complexes) is observed in the GaP epitaxial films [8]. Surface H allows the surface to satisfy the ECR [15]. The clean GaP(001)-(2 × 2) model surfaces discussed above do not satisfy the ECR. This provides a thermodynamic driving force for H to incorporate into the film.

In order for the GaP(001)-(2 × 2) surface to satisfy the ECR, one H can be added to each surface dimer on alternating sides, causing dimer buckling. This has been shown by our calculations to have the lowest energy [13]. When Sb is incorporated as a surfactant, the H bonds to the Sb dimers in the same way (see Fig. 2d), because Sb is isoelectronic with P. Thus, to investigate the role of H, we calculated the film doping energy with surface H. First, we tested the situation with two surface H/cell without Sb (Fig. 2c). Assuming that the H coverage remained the same, with two H atoms before and after dopant incorporation. Previously for Zn doping we found $\Delta E_{1st}^{P-2H \rightarrow 2H} = 2.68\text{ eV} + \mu_{Ga} - \mu_{Zn}$ [13], which is 0.22 eV higher than the case without H, as shown in Fig. 2c vs. a. This shows that without Sb, H alone does not enhance the doping. This film doping energy difference is defined as ΔE_2 in Table 2. We believe that this is largely because the ECR is satisfied before doping, but violated after doping. Here, for the other p-type dopants studied, we found a similar trend. The film doping energies for the case with H for Mg, Cd and Be are, respectively, 0.07, 0.55 and 0.41 eV higher than the case without H, listed as ΔE_2 in Table 2. So we concluded that when H is introduced into the system without Sb, the film doping energy for the p-type dopants doesn't drop.

Next, we investigated the combined effects of Sb and H. Assuming again a surface covered with 2H/cell before and after the p-type dopant incorporation (see Fig. 2d), we previously found that for the case of Zn, $\Delta E_{1st}^{Sb-2H \rightarrow 2H} = 1.75\text{ eV} + \mu_{Ga} - \mu_{Zn}$ [13]. Clearly, the Zn film doping energy is substantially reduced, by 0.78 eV, relative to the bare Sb-terminated surface without H from Fig. 2b to d (defined as ΔE_3 in Table 2) and by 0.93 eV relative to the H-covered P-terminated surface without Sb from Fig. 2c to d (defined as ΔE_4 in Table 2). We have termed this intriguing observation the “dual-surfactant” effect of Sb and H: *the two surfactants work together in a constructive manner to lower the Zn film doping energy, while they do not lower the Zn film doping energy individually*. For other p-type dopants, we found a similar trend. As shown by the values of ΔE_3 and ΔE_4 in Table 2, the film doping energy for Mg with both Sb and H is 0.47 eV lower than the case with only Sb and 0.69 eV lower than the case with only H. The film doping energy for Cd with both Sb and H is 0.49 eV lower than the case with only Sb, and 0.85 eV lower than case with only H. The film doping energy for Be with both Sb and H is 0.92 eV lower than the case with only Sb and 0.97 eV lower than the case with only H. So the dual surfactant effect can be extended to all the p-type dopants studied: *the surfactants Sb and H work together in a constructive manner to lower the p-type film doping energy for a wide range of acceptor elements residing on the group III sublattice*.

The above results indicate that the surfactant effect of Sb is enhanced when surface H is also introduced. The underlying physical reason giving rise to the effect of Sb is probably due to the lower electronegativity of Sb in comparison with P. In a similar spirit to the generalized ECR in the semiconductor surface with metal elements proposed recently [14]. Antimony is more metallic than P, so that Sb can serve more effectively as an electron reservoir to accommodate the redistribution of electrons when a p-type dopant is present. Since the p-type dopant will violate the ECR by having one less electron, it is easier for Sb than for P to accommodate the missing electron in order to “partially” satisfy the ECR. Also, we can see that the dual surfactant effect in decreasing the film doping energy is smallest for Mg, compared with the other three elements. This is probably due to the electronegativity difference among these dopants. Mg, Be, Cd and Zn have electronegativities of 1.31, 1.57, 1.69, 1.65, respectively [25]. So the electronegativity of Mg is noticeably the lowest among all these four elements. Thus, relatively more electrons of Mg can contribute to the electron redistribution, and the dopant Mg itself can be considered as an electron reservoir which might negate part of the electron reservoir effect that Sb contributes to the system. Consequently, Sb and H have the smallest dual surfactant effect for Mg incorporation.

Next, we investigated the surface configuration with three surface hydrogen atoms per four Sb atoms. The ECR is violated after the dopant is incorporated if the surface H remains constant. In order to satisfy the ECR, one additional H has to be added. In our previous study of Zn, to quantify the role of the extra H, we calculated the Zn film doping energy by assuming a surface covered with 2H before, but with 3H after doping (see Fig. 4b–c). We found that $\Delta E_{1stZn}^{Sb-2H \rightarrow 3H} = -0.63 \text{ eV} + \mu_{Ga} - \mu_{Zn} - \mu_H = 0.04 \text{ eV} + \mu_{Ga} - \mu_{Zn}$ [13] (note that the value is different from Ref. [13] due to a different μ_H used here. The same is true for doping whenever μ_H appears in the rest of the paper). Clearly, by adding an extra H after doping to satisfy the ECR, the film doping energy of the Zn can be decreased further depending on the H chemical potential (μ_H). Here, we examine the effect of the third H for the case of Mg/Cd/Be, and find that $\Delta E_{1stMg}^{Sb-2H \rightarrow 3H} = -0.91 \text{ eV} + \mu_{Ga} - \mu_{Zn} - \mu_H = -0.24 \text{ eV} + \mu_{Ga} - \mu_{Mg}$, $\Delta E_{1stCd}^{Sb-2H \rightarrow 3H} = 0.84 \text{ eV} + \mu_{Ga} - \mu_{Cd}$ and $\Delta E_{1stBe}^{Sb-2H \rightarrow 3H} = -2.38 \text{ eV} + \mu_{Ga} - \mu_{Be}$, respectively. So once again, the film doping energy of Mg/Cd/Be can be further decreased depending on the chemical potential of H. Since the chemical potential of H we use here is the lower limit, in the actual growth, we expect a larger doping energy drop.

So far, we have shown the dual-surfactant effect of Sb and H in enhancing the p-type doping in the first cation layer, i.e., the surface position. It is also important to investigate the configuration where the dopant replaces a Ga atom at the second cation layer, i.e., the subsurface or “bulk” position. In our previous study

of Zn, we considered two possible configurations: one with Zn in the second cation layer between two surface Sb dimers (Fig. 3a) and the other directly below the surface Sb dimers (Fig. 3b). The respective film doping energies were $\Delta E_{2ndZn,between}^{Sb-2H \rightarrow 3H} = 0.13 \text{ eV} + \mu_{Ga} - \mu_{Zn}$ and $\Delta E_{2ndZn,below}^{Sb-2H \rightarrow 3H} = 0.21 \text{ eV} + \mu_{Ga} - \mu_{Zn}$ [13]. The 0.08 eV difference between the two reflects the dependence of Zn film doping energy on the “atomic-level” stress at these sites [26] and Zn is slightly favored at the tensile sites between surface dimers relative to the compressive sites directly below surface dimers. Here, we have expanded this treatment to include Mg/Cd/Be and found a similar result. The respective film doping energies are: $\Delta E_{2ndMg,between}^{Sb-2H \rightarrow 3H} = 0.3 \text{ eV} + \mu_{Ga} - \mu_{Mg}$ and $\Delta E_{2ndMg,below}^{Sb-2H \rightarrow 3H} = 0.58 \text{ eV} + \mu_{Ga} - \mu_{Mg}$; $\Delta E_{2ndCd,between}^{Sb-2H \rightarrow 3H} = 1.1 \text{ eV} + \mu_{Ga} - \mu_{Cd}$ and $\Delta E_{2ndCd,below}^{Sb-2H \rightarrow 3H} = 1.46 \text{ eV} + \mu_{Ga} - \mu_{Cd}$; $\Delta E_{2ndBe,between}^{Sb-2H \rightarrow 3H} = -2.25 \text{ eV} + \mu_{Ga} - \mu_{Be}$ and $\Delta E_{2ndBe,below}^{Sb-2H \rightarrow 3H} = -2.31 \text{ eV} + \mu_{Ga} - \mu_{Be}$. The 0.28 eV energy difference between the two sites for Mg and 0.36 eV energy difference between the two sites for Cd, which are larger than that of Zn are probably due to the larger covalent radii of Mg and Cd [27]. So the tensile site is even more favored by a larger Mg and Cd. Be is slightly favored at the compressive site, which is due to the smaller covalent radius of Be.

Lastly, we have investigated co-doping of the p-type dopant and H into the GaP bulk. Experimental observation indicated that complexes of Zn, P and H form during doping of Zn in GaP [28]. This suggests some H goes into the bulk with the acceptor. In our previous Zn study, we calculated the energies associated with one H incorporation into the subsurface with Zn, and determined the Zn–P–H complex structures. Fig. 3c shows the doping of a Zn atom in the subsurface (or “bulk”) position along with an H atom next to it. There will be 2 H atoms remaining on the surface (in comparison to 3H in Fig. 3a), so that the ECR is still satisfied.

When a surface H goes into the subsurface, it changes the dopant bonding configuration, forming a dopant–P–H complex. Without H, the dopant bonds with four neighboring P atoms in an sp^3 hybridization (a tetrahedral structure, Fig. 3a). With the extra H, one dopant–P bond is broken to form a P–H bond, and the dopant bonds with three neighboring P atoms in an sp^2 hybridization (a planar structure, Fig. 3c). This can also be explained by the ECR. The dopant provides two valence electrons and the H provides one. For both P–H and P–dopant bonds, this takes $\frac{3}{4}$ electrons, so their sum gives three electrons total to satisfy the ECR. Thus, when H is co-doped with the dopant, it changes the dopant bonding configuration from sp^3 to sp^2 hybridization, forming three dopant–P bonds plus an empty orbital.

The co-doping of H with dopant into the subsurface is also found to be energetically favorable. The film doping energy at the 2nd-cation-layer positions forming the Zn–P–H complex was found previously to be $\Delta E_{2ndZn}^{Sb-2H \rightarrow 1bulkH} = -0.19 \text{ eV} + \mu_{Ga} - \mu_{Zn}$

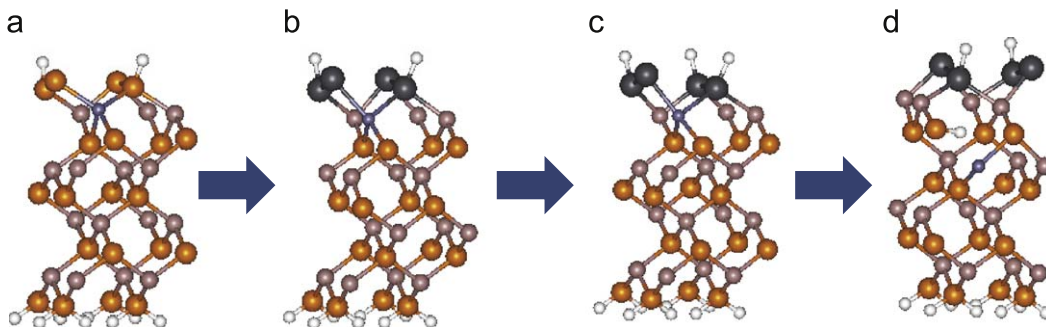


Fig. 4. (Color online) Schematic illustration of a plausible doping process, with one Mg(Zn) atom replacing a Ga atom in GaP film. Atom labels are the same as in Fig. 1. (a) Mg(Zn) doped into the first cation layer with surface P dimers. (b) Mg(Zn) doped into the first cation layer replacing Ga with surface Sb dimers. (c) One additional H is added onto the surface to satisfy ECR. (d) H co-doped with Mg(Zn) into the 2nd cation layer to form a Mg(Zn)–P–H complex.

[13], which is about 0.2 eV lower than the corresponding cases with all 3H atoms remaining on the surface. This suggests that there exists a thermodynamic driving force for one H atom to go into the subsurface (or “bulk”) with the dopant, i.e. co-doping of the Zn with H. We have further performed the 2nd cation layer Mg/Cd/Be doping calculation. The film doping energy is $\Delta E_{2nd,Mg}^{Sb-2H \rightarrow 1bulkH} = -0.29 \text{ eV} + \mu_{Ga} - \mu_{Mg}$, $\Delta E_{2nd,Cd}^{Sb-2H \rightarrow 1bulkH} = 0.80 \text{ eV} + \mu_{Ga} - \mu_{Cd}$ and $\Delta E_{2nd,Be}^{Sb-2H \rightarrow 1bulkH} = -2.59 \text{ eV} + \mu_{Ga} - \mu_{Be}$. All the energies are lower than the corresponding case with all 3H atoms on the surface. So, similar to H co-doping with Zn into the bulk, it is confirmed that there is a thermodynamic driving force for one H atom to go into the bulk with Mg/Cd/Be. On the other hand, it is known that H would compensate the p-type dopant in bulk GaP, mitigating the doping effect [29,30], which is also confirmed by our electronic structure calculations. To activate the acceptor, annealing can be done after the doping process to remove the H [29,30]. In other words, the co-doped H must be removed after it serves its purpose to assist the dopant incorporation.

Now, based on all the above calculations, we postulate a plausible complete p-type doping process during OMVPE growth, the same as the Zn doping process [13] in GaP, driven by the dual surfactant effect of Sb and H as shown in Fig. 4 for Mg as an example. The doping of Mg in the original P-terminated surface covered with 2H/cell is shown in Fig. 4a. In the first step, with Sb always replacing the P dimers, a Mg atom is added into the first cation layer (Fig. 4b), where it assists the doping process. Two surface H atoms allow the ECR to be satisfied before doping and Sb plays the role of providing an electron reservoir to accommodate the redistribution of electrons when the ECR is violated after the key step involving exchange of surface Mg and Ga from the lattice. In a subsequent step, one additional H is added to the surface to further assist the doping process by adding one more electron to satisfy the ECR (Fig. 4c). In the third step, the Mg atom goes into the subsurface (“bulk”) and replaces a Ga atom in the 2nd or lower cation layers. Simultaneously, a surface H goes together with Mg into the subsurface (“bulk”) as a co-dopant to form a Mg–P–H complex, as shown in Fig. 4d, where the ECR is satisfied both at the surface and in the bulk at the complex site. The co-doped H needs to be removed later by annealing to activate the acceptor.

The corresponding film doping energy changes are shown in Fig. 5 for the case of Zn, Mg, Cd and Be. The squares are for Zn. The first step has $\Delta E = -0.93 \text{ eV}$, showing the energy difference between the Sb/2H enhanced system and P/2H system. The second step has $\Delta E = -1.71 \text{ eV}$, showing the energy difference between the Sb/3H system and Sb/2H system. The third step has $\Delta E = -0.23 \text{ eV}$, showing the energy difference between the P–Zn–H complex and Sb/3H system. For Mg (circle)/Cd (triangle)/Be (star), the first step has $\Delta E = -0.69, -0.85$ and -0.97 eV , respectively, reflecting the role of Sb and 2H as dual surfactants; the second step has $\Delta E = -1.82, -1.65$ and -1.83 eV , respectively, reflecting the role of the third H (also, in the growth chamber, due to the higher chemical potential of H than our estimated value, the doping energy drop will be greater than our calculated result); the third step has $\Delta E = -0.05, -0.04$ and -0.2 eV , reflecting the energy gain in forming P–Mg/Cd/Be–H complex. Consequently, we have an overall downhill energy landscape for the whole doping process thermodynamically. Notice that the second-step film doping energy with one H added to the system depends on the H chemical potential, while the third-step H film co-doping energy with one H moving from surface to bulk does not. This implies that one may increase the partial pressure of H and hence H chemical potential during growth to further enhance p-type doping in the second step. Also, we predict that the dual surfactant effect is the strongest for Be and weakest for Mg and Cd, which still needs further experimental work to prove.

Our theoretical picture of the dual-surfactant effect and its underlying physical mechanism based on the ECR is qualitatively consistent with the experimental observation of both the enhanced Zn doping with Sb introduction during OMVPE growth and the co-incorporation of H with Zn [7,8]. However, because the computation is limited to a small cell size, we can only calculate a few representative cases of surface structures, surface coverage, and dopant concentrations. Therefore, the actual energy values may vary with these conditions and should be treated with caution. However, the overall trend of the calculated energy changes is expected to be generally correct. Also, other factors, such as temperature and kinetic rates of atom exchange and incorporation, need to be taken into account in future studies in order to obtain a more complete picture of the dual-surfactant effect. For example, from the energy scales shown in Fig. 5, temperature is expected to have a lesser effect on the Zn and Mg film doping energy (1.0, 0.7 eV in step 1) than on the H film co-doping energy (0.2, 0.05 eV in step 3). However, changing temperature will change surface H coverage which will in turn affect film doping energy. The kinetic barriers associated with each step of the process are also important, but their calculations would go beyond the scope of this work which focuses on the thermodynamic aspects of film doping energies and the underlying physical principles based on ECR. Entropy also enters the free energy calculation. At high temperature limit, the vibrational entropy can be approximated as $S = 3R[\ln(T/T_{Debye}) + \frac{4}{3}]$ [31], where, T_{Debye} is the Debye temperature, which is 445 K for GaP [32]. At 900 K, the entropy is 50.5 J/kmol. However, the entropy effect is canceled in the calculation of the change of doping energy due to the surfactant effect.

In conclusion, we have discovered an interesting dual-surfactant effect of Sb and H for p-type doping enhancement for Zn, Cd, Mg and Be. The dual-surfactant with two surface elements will greatly broaden the scope and application of the conventional surfactant effect with one surface element. The two surface H atoms serve as part of the dual surfactant effect and the H in the bulk serves as a co-dopant. Specifically, in order to accommodate the p-type dopant incorporation, the role of the surfactant Sb (a “metallic” element) is to provide an electron reservoir to

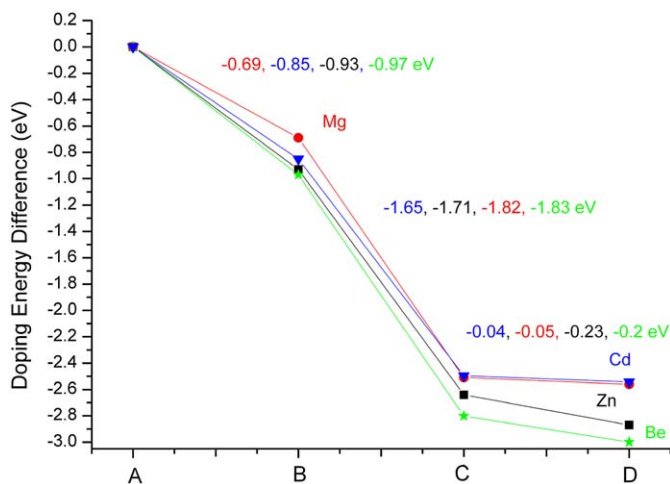


Fig. 5. Change of doping energy at each doping step as shown in Fig. 4. Square (black): Zn as dopant; circle (red): Mg as dopant. Triangle (blue): Cd; star (green): Be. (For interpretation of the references to color in this figure legend, the reader is referred to the web version of this article.)

redistribute electrons, while the role of the two surfactant H is to satisfy the ECR at the surface before doping, and the co-doped H (a “single electron”) is to add one electron to satisfy ECR in the bulk after the doping. Later annealing allows the codoped H to diffuse away. We believe the dual-surfactant effect we disclose here can be used as a general strategy for enhancing p-type doping of III–V semiconductors by using a metallic-element with H as dual-surfactants and co-dopants.

The authors are grateful to DOE-BES for supporting this work. The calculations were performed on AMD Opteron cluster at the CHPC, University of Utah. We thank Anil Virkar for helpful discussions.

References

- [1] M. Copel, M.C. Reuter, E. Kaxiras, R.M. Tromp, *Phys. Rev. Lett.* 63 (1989) 632.
- [2] G. Rosenfeld, et al., *Phys. Rev. Lett.* 71 (1993) 895.
- [3] J. Meyer, J. Vrijmoeth, H. van der Vegt, R. Behm, *Phys. Rev. B* 51 (1995) 14790.
- [4] M.R. Pillai, S.-S. Kim, S.T. Ho, S.A. Barnett, *J. Vac. Sci. Technol. B* 18 (2000) 1232.
- [5] E. Rudkevich, F. Liu, D.E. Savage, T.F. Kuech, L. McCaughan, M.G. Lagally, *Phys. Rev. Lett.* 81 (1998) 3467.
- [6] C.M. Fetzner, R.T. Lee, J.K. Schurtleff, G.B. Stringfellow, S.M. Lee, T.Y. Seong, *Appl. Phys. Lett.* 76 (2000) 1440.
- [7] D.C. Chapman, A.D. Howard, G.B. Stringfellow, *J. Crystal Growth* 287 (2006) 647.
- [8] A.D. Howard, D.C. Chapman, G.B. Stringfellow, *J. Appl. Phys.* 100 (2006) 44904.
- [9] R.R. Wixom, L.W. Rieth, G.B. Stringfellow, *J. Crystal Growth* 265 (2004) 367–374.
- [10] W. Shockley, J.L. Moll, *Phys. Rev.* 119 (5) (1960) 1480.
- [11] S.J. Pearton, H. Cho, F. Ren, J.I. Chyi, J. Han, R.G. Wilson, in: R. Feenstra, T. Myers, M.S. Shur, H. Amano (Eds.), *GaN and Related Alloys*, vol. 595, Materials Research Society, 2000, pp. W10.6.1–W10.6.10.
- [12] J.K. Shurtleff, S.W. Jun, G.B. Stringfellow, *Appl. Phys. Lett.* 78 (2001) 3038.
- [13] J.Y. Zhu, F. Liu, G.B. Stringfellow, *Phys. Rev. Lett.* 101 (2008) 196103.
- [14] L. Zhang, E.G. Wang, Q.K. Xue, S.B. Zhang, Z. Zhang, *Phys. Rev. Lett.* 97 (2006) 126103.
- [15] P.K. Larsen, D.J. Chadi, *Phys. Rev. B* 37 (1988) 8282.
- [16] S.D. Burnham, G. Namkoong, W. Henderson, W.A. Doolittle, *J. Crystal Growth* 279 (2005) 26–30.
- [17] G. Kresse, J. Hafner, *Phys. Rev. B* 49 (1994) 14251; G. Kresse, J. Furthmüller, *Comput. Mater. Sci.* 6 (1996) 15.
- [20] R. Wixom, N.A. Modine, G.B. Stringfellow, *Phys. Rev. B* 67 (2003) 115309.
- [21] C.G. Van de Walle, J. Neugebauer, *Phys. Rev. Lett.* 88 (2002) 066103.
- [22] O. Knacke, O. Kubaschewski, K. Hesselmann (Eds.), *Thermochemical Properties of Inorganic Substances*, second Ed., Springer-Verlag, 1991, pp. 728, 743, 803.
- [23] G. B. Stringfellow, *Organometallic Vapor-Phase Epitaxy, Theory and Practice*, second ed., Academic Press, 1999, pp. 141, 243.
- [24] M. Sugiyama, S. Maeyama, F. Maeda, M. Oshima, *Phys. Rev. B* 52 (1995) 2678.
- [25] A.L. Allred, J. Inorg. Nucl. Chem. 17 (1961) 215.
- [26] F. Liu, M.G. Lagally, *Phys. Rev. Lett.* 76 (1996) 3156.
- [27] B. Cordero, V. Gmez, A.E. Platero-Prats, M. Revs, J. Echeverra, E. Cremades, F. Barragn, S. Alvarez, *Dalton Trans.* 2008 (2008) 2832–2838.
- [28] M.D. McCluskey, E.E. Haller, J.W. Walker, N.M. Johnson, *Appl. Phys. Lett.* 65 (1994) 2191.
- [29] E.V.K. Rao, B. Theys, Y. Gottesman, H. Bissessur, in: 11th International Conference on Indium Phosphide and Related Materials, IEEE, 0-7803-5562-8/99, 1999.
- [30] C.H. Chen, S.A. Stockman, M.J. Peanasky, C.P. Kuo, in: G.B. Stringfellow, M.G. Craford (Eds.), *Semiconductors and Semimetals*, vol. 48, Academic Press, New York, 1997, pp. 122–127.
- [31] M.D. Sturge, *Statistical and Thermal Physics: Fundamentals and Applications*, illustrated ed., A K Peters, Ltd., 2003, p. 136.
- [32] M. Ilegems, H.C. Montgomery, *J. Phys. Chem. Solids* 34 (1973) 885.